Effects of oligoDNA template length and sequence on binary self-assembly of a nucleotide bolaamphiphile

Rika Iwaura,*[a] Yoshihiro Kikkawa,[b] Mayumi Ohnishi-Kameyama[a] and Toshimi Shimizu*[b,c]

Received 31st July 2007, Accepted 17th September 2007
First published as an Advance Article on the web 1st October 2007
DOI: 10.1039/b711687j

Templated self-assembly of nucleotide bolaamphiphile **1** (in which a 3′-phosphorylated thymidine moiety is connected to each end of a long oligomethylene chain) with a 10-, 20-, 30-, or 40-meric single-stranded oligoadenylic acid (**2**, **3**, **4**, or **5**) led to the formation of right-handed helical nanofibers in 0.1× Tris/EDTA (TE) buffer solutions. The helical pitch increased as the length of the oligoadenylic acid template increased. DNA composed of oligoadenylic and oligocytidylic acid sequences (**6**, **7**, and **8**) also acted as templates to induce the formation of helical nanofiber structures. The diameter of the nanofibers remained constant (6–6.6 nm) irrespective of the template used. The binary self-assembly of **1** with **4** also produced higher-order, double-stranded nanofibers.

Introduction

In biological systems such as DNA, molecular recognition between building block molecules and subsequent self-assembly of those molecules play substantial roles. For example, DNA molecules form a variety of structures that are based on complementary base pairing and double helix formation. Researchers in the field of supramolecular chemistry have developed sophisticated biomolecular systems, such as supramolecular polymers,[1] liquid-crystalline assemblies,[2] fibers,[3] and tubes,[4] by using molecular recognition between and self-assembly of synthetic molecules.[5] These supramolecular assemblies occasionally produce hierarchical structures, such as columnar,[6] coiled-coil,[7] and membrane structures.[8] In addition, researchers have found that DNA functions well as a template to align organic and inorganic compounds by means of noncovalent interactions. For example, electrostatic interaction between anionic DNA and cationic compounds facilitates the arrangement of lipids[9] and metals.[10] Biotinylated oligonucleotides can act as scaffolds to make protein arrays,[11] and metal–ligand interactions allow for the construction of metal arrays in artificial DNA.[12] Complementary base pairing is also useful for organizing metal particles,[13] metallosalens,[14] crown ethers,[15] and conjugated molecules.[16] For example, Shinkai *et al.*[17] and Schenning *et al.*[18] have reported that the one-dimensional self-assembly of lipids and chromophores that possess complementary hydrogen bonding sites can be templated by polyadenylic acid [poly(A)] and by 40-meric oligothymidylic acid [dT_{40}], respectively. We found that the self-assembly of bola-shaped molecules with a complementary oligoadenylic acid [$d(A)_n$, where $n = 10$, 20, or 40] template forms unique DNA-like nanofibers.[19,20] Although there are many recent examples of DNA-templated systems, little attention has been paid to the effect of the DNA-template length on the self-assembled morphologies. Here we describe detailed atomic force microscopy (AFM) studies of the effect of oligonucleotide template length on the dimensions of nanofibers self-assembled from nucleotide bolaamphiphile **1** (Scheme 1). In particular, we focused on the how the helical pitch, diameter, and higher-order structures of the nanofibers varied depending on the number of bases and the sequence of oligonucleotide templates **2–8**.

Results and discussion

Effect of oligoadenylic acid template length

Binary self-assembly of **1** in 0.1× Tris/EDTA (TE) buffer solutions with single-stranded oligoadenylic acids **2–5** produced nanofiber structures through the formation of complementary thymine–adenine base pairs.[20,21] Precise AFM analysis of the nanofibers indicated that the helical pitch of the binary self-assembly increased as the length of the oligoadenylic acid template increased. The binary self-assembly of **1** with **2** (abbreviated **1/2**, hereafter) resulted in helical nanofiber structures 1 day after the compounds were combined. After a week, we observed wavy nanofiber morphologies with a 160 nm pitch and a 6.4 nm diameter, along with nonwavy nanofibers (Fig. 1a). The section profile of the surface of the wavy nanofibers showed a periodically rugged surface with an 11 nm pitch (Fig. 2a and b), suggesting a right-handed helical structure, which is consistent with the results obtained by circular dichroism spectroscopy. Binary self-assembly of **1** with **3** produced similar nanofiber structures with a 6.4 nm diameter and a periodically rugged surface with an 18 nm pitch (Fig. 1b, 2c and d). Transmission electron microscopy (TEM) revealed a 20 nm pitch for the **1/3** self-assembly prepared in water,[20] and this value is similar to that observed by AFM. When the template length was increased, the helical pitches of the resulting binary self-assemblies were 24 and 40 nm for **1/4** (Fig. 2e and f) and **1/5** (Fig. 2g and h), respectively. Similarly, we observed nanofiber

[a]*National Food Research Institute (NFRI), National Agriculture and Food Research Organization (NARO), 2-1-12 Kannondai, Tsukuba, Ibaraki, 305-8642, Japan. E-mail: riwaura@affrc.go.jp; Fax: +81 29 838 7996; Tel: +81 29 838 7154*
[b]*Nanoarchitectonics Research Center (NARC), National Institute of Advanced Industrial Science and Technology (AIST), Tsukuba Central 5, 1-1-1 Higashi, Tsukuba, Ibaraki, 305-8565, Japan. E-mail: tshmz-shimizu@aist.go.jp; Fax: +81 29 861 4545; Tel: +81 29 861 4544*
[c]*SORST, Japan Science and Technology Agency (JST), Tsukuba Central 5, 1-1-1 Higashi, Tsukuba, Ibaraki, 305-8565, Japan*

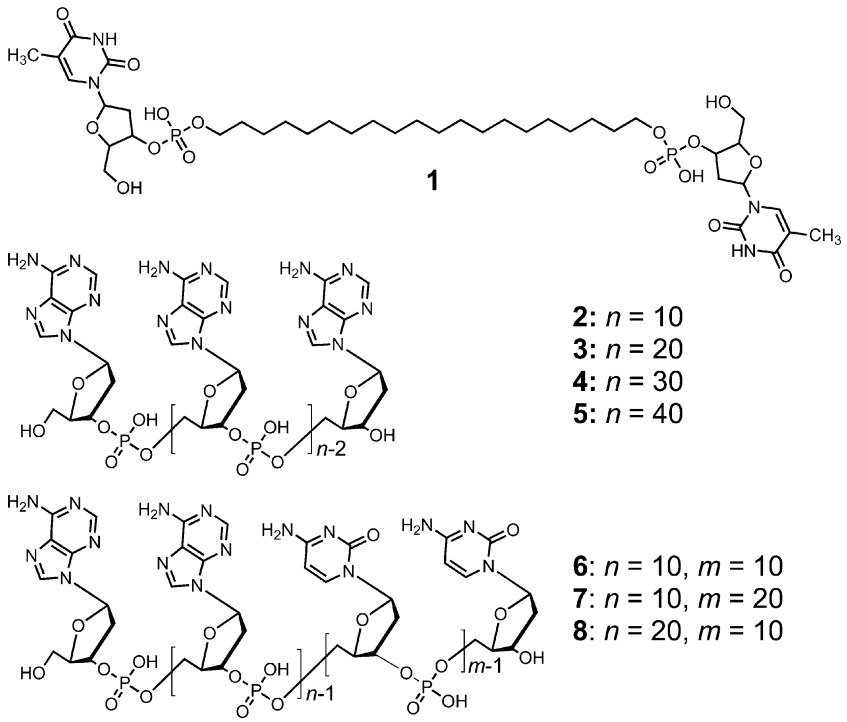

Scheme 1

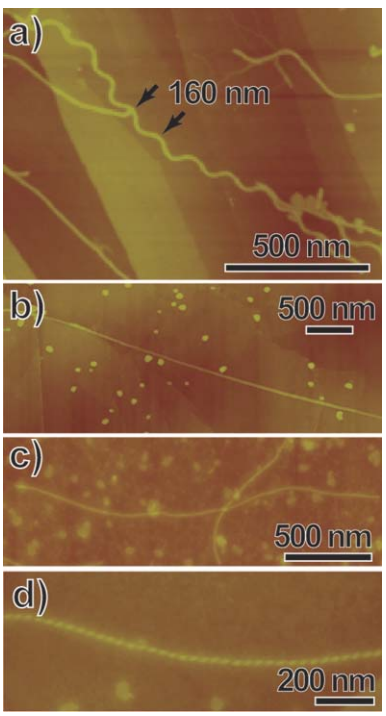

Fig. 1 AFM images of (a) **1/2**, (b) **1/3**, (c) **1/4**, and (d) **1/5** produced in 0.1× TE buffer solutions on highly oriented pyrolytic graphite (HOPG).

structures with diameters of 6.4 and 6.6 nm for **1/4** and **1/5**, respectively (Fig. 1c and d). The observed diameters for the helical nanofibers formed from **1/2**, **1/3**, **1/4**, and **1/5** were compatible with the proposed structure, in which an oligoadenylic acid moiety is hydrogen bonded to each end of the nucleotide bolaamphiphile (molecular length = 3.5 nm), as described elsewhere.[20,22]

UV-vis and circular dichroism (CD) spectroscopy

UV-vis and circular dichroism (CD) spectra provide much information about the interaction between nucleobases and conformation of DNA molecules.[23] The CD spectra of double-stranded polydeoxynucleotides carrying adenine–thymine repeating units have been precisely studied and found to feature curved or bent DNA regions that are important in biological systems.[24–26,27] UV-vis and CD spectroscopic measurements of the binary self-assemblies of **1** and oligoadenylic acids **2–5** revealed that the geometries of the base pairs strongly depended on the length of the DNA template used. CD spectra of the binary self-assemblies in 0.1× TE buffer solutions showed a positive Cotton effect, suggesting a right-handed helicity in the nucleobase moieties of **1** and oligoadenylic acids **2–5**.[28] Interestingly, the CD patterns depended on the length of the oligoadenylic acid used (Fig. 3a). B-DNA predominates in cells and is formed from double-stranded polydA·dT or polyd(A–T)·polyd(A–T).[26] The CD spectra of **1/2** and **1/4** were distinct from the spectrum of B-DNA. In particular, the CD spectrum of **1/2** gave two positive bands, at $\lambda = 275$ and 257 nm, as well as a negative band at $\lambda = 244$ nm with a zero crossing at $\lambda = 255$ nm. This spectral pattern closely resembles that of double-stranded poly[d(A_nT_n)]·poly[d(A_nT_n)] (n = 3, 5, 6). In addition, this spectral pattern is attributable to the large propeller twist[25] (the angle between the planes of the hydrogen-bonded base pairs) between the base pairs. In the spectra of **1/3** and **1/5**, we observed bisignated CD bands with a positive Cotton band, a negative Cotton band, and a zero crossing at 265, 247, and 255 nm, respectively. A similar CD pattern has been reported for a double-stranded poly[d(A_2T_2)]·poly[d(A_2T_2)], in which the A–T base pairs have propeller twists smaller than those of poly[d(A_nT_n)]·poly[d(A_nT_n)] ($n > 2$), which has longer A–T repeating units. Furthermore, these CD spectra indicate that

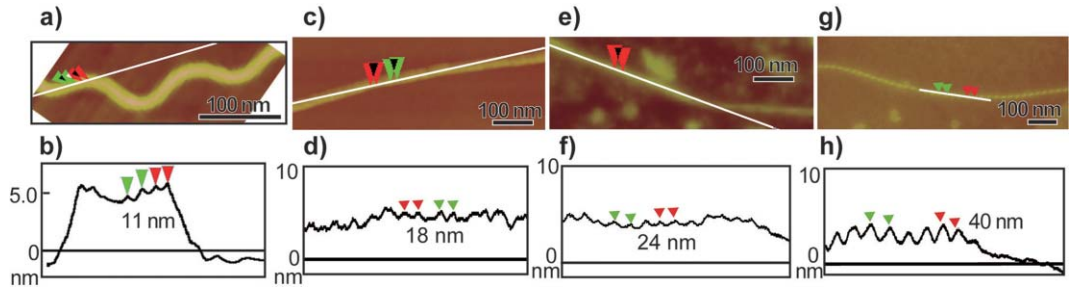

Fig. 2 AFM images and section profiles of (a,b) **1/2**, (c,d) **1/3**, (e,f) **1/4** and (g,h) **1/5**. The AFM images were taken 1 week after preparation of the self-assemblies.

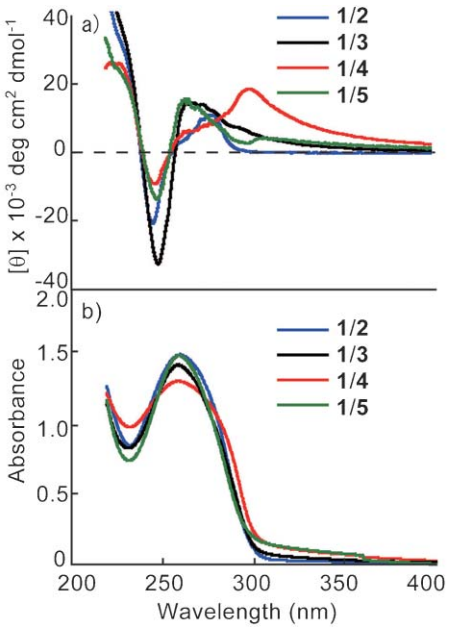

Fig. 3 (a) CD and (b) UV-vis spectrum of **1/2**, **1/3**, **1/4**, and **1/5** produced in 0.1× TE buffer solutions at 20 °C ([**1**] = 2.6 × 10^{-3} mol dm^{-3}).

1/3 and **1/5** take similar conformations in the helical nanofibers. The CD spectrum of **1/4** gave two positive bands, at $\lambda = 297$ and 260 nm, and a negative band at $\lambda = 245$ nm with a zero crossing at $\lambda = 255$ nm, suggesting a higher-order structure, which will be discussed later. In addition, the intensity of the absorption maxima for **1/4** at $\lambda = 258$ nm decreased by 14% relative to the intensities of the maxima for **1/2**, **1/3**, and **1/5** (Fig. 3b).

The effect of the oligonucleotide template sequence

To determine how the fiber morphology depended on the sequences of the DNA templates, we also examined the binary self-assemblies of **1** with oligonucleotides **6**, **7**, and **8**, which are related to one another. Nucleotides **6**, **7**, and **8** have complementary oligoadenylic acids and noncomplementary oligocytidylic acids at the 5′- and 3′-ends, respectively. The lengths of the complementary and noncomplementary regions vary: 10-mer/10-mer, 10-mer/20-mer, and 20-mer/10-mer for **6**, **7**, and **8**, respectively. The helical pitches of the resultant nanofibers depended on the length of the complementary region, but not on the length of the noncomplementary region. Binary self-assemblies **1/6** and **1/7** produced nanofiber structures with 6.1 nm diameter and 12 nm pitch (Fig. 4a–c) and with 6.0 nm diameter and 11 nm pitch (Fig. 4d, c and f), respectively; these values are similar to those for **1/2**. All the templates for these binary self-assemblies have 10 complementary adenine moieties in the base sequence. In contrast, the binary self-assembly of **1** with oligonucleotide **8**, which has 20 adenylic acids and 10 cytidylic acids, produced wavy morphology coexisting with a stranded rope (Fig. 5i).

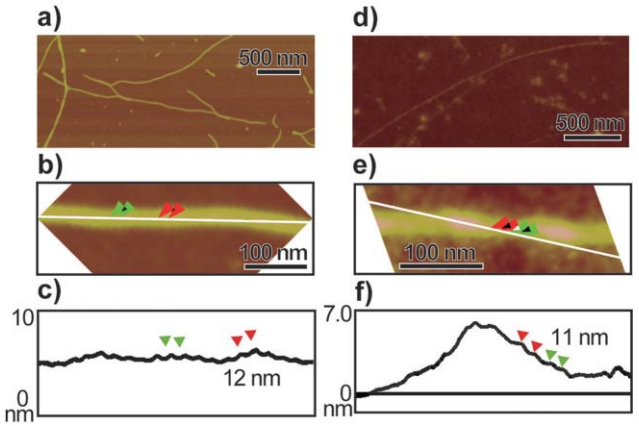

Fig. 4 AFM images of (a,b) **1/6** and (c) the section profile in (b). AFM images of (d,e) **1/7** and (f) the section profile in (e).

Higher-order structures of the binary self-assemblies

When the binary self-assemblies templated by the 30-meric oligonucleotides (**4**, **7**, **8**) were aged for several weeks, higher-order structures of helical nanofibers with relatively longer pitches were produced. Binary self-assembly **1/4** gave partially stranded rope structures with a pitch of 100 nm (Fig. 5a, c, and 6). The three-dimensional image of **1/4** revealed the right-handed helicity of the stranded rope (Fig. 6b). Interestingly, the morphology around the terminal region of the stranded rope was different than the morphology of the rest of the rope: a nanofiber that was thinner (6.4 nm) than the stranded rope (12 nm high) was observed at the terminal region (Fig. 5c, d, and 6a). This observation indicates that two self-assembled helical nanofibers were formed by the binary self-assembly of **1** and **4**, which resulted in the double-stranded rope structure. We were able to determine that the periodicity was 11 nm, on the basis of the section profile along the long axis of the stranded rope (Fig. 5e, f). Similar helical nanofibers having a pitch of approximately 100 nm were also observed for **1/7** and **1/8** (Fig. 5g, h, and i) after the assemblies were aged for several weeks.

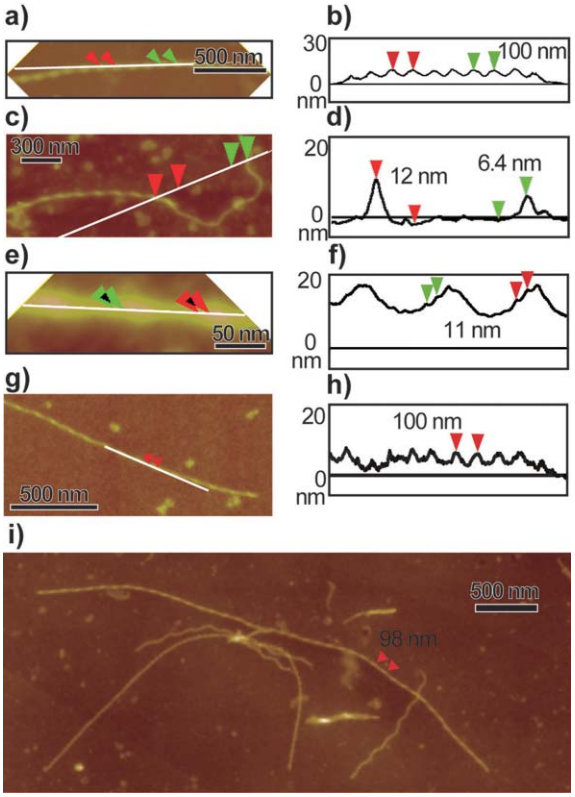

Fig. 5 (a, c, e) AFM images of **1**/**4** and (b, d, f) the corresponding section profiles. (g) AFM image of **1**/**7** and (h) the section profile in (g). (i) AFM image of **1**/**8** with various morphologies.

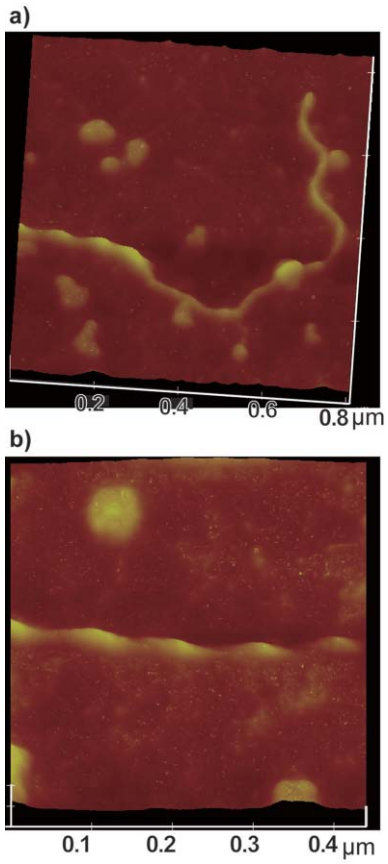

Fig. 6 Three-dimensional images of (a) the terminal region and (b) the center of the double-stranded rope self-assembled from **1** and **4**.

Proposed structures and binary self-assembly mechanisms

The AFM observations combined with UV-vis and CD spectra strongly suggest that the binary self-assembly of **1** and compounds **2–8** resulted in a variety of helical nanofiber morphologies depending on the length and sequence of the oligonucleotide used (Table 1).

The helical pitch of the nanofibers increased as the length of the oligoadenylic acid template increased (Table 1, Fig. 7a). Generally, the DNA double helix has a stable and robust structure due to complementary base pairing. However, the base pairing interaction is sometimes disrupted. A phenomenon called end fraying has been reported, in which hydrogen bonds break and eventually a base pair becomes free at the terminus of the helix.[29] Binary self-assemblies with relatively short templates, such as **2**, can be expected to exhibit more end fraying than assemblies with

Table 1 The structural properties of the binary self-assemblies

	Template		Self-assembled morphology		
Composition	Total length[a]	Complementary bases[b]	Pitch/nm	Diameter/nm [d]	Higher-order structure
1/**2**	10	10	helical fiber		wavy fiber[e]
			11	6.4	pitch = 160 nm
1/**3**	20	20	helical fiber		—
			18	6.0	
1/**4**	30	30	helical fiber		double-stranded rope[f]
			24	6.4	pitch = 100 nm
1/**5**	40	40	helical fiber		
			40	6.6	
1/**6**	20	10	helical fiber		
			12	6.1	—
1/**7**	30	10	helical fiber		double-stranded rope[g]
			11	6.0	pitch = 100 nm
1/**8**	30	20	helical fiber		double-stranded rope[h]
			—[c]	6.7	pitch = 99 nm

[a] Number of bases in the oligonucleotide template. [b] Number of complementary bases in the oligonucleotide template. [c] Not determined. [d] The diameters of the nanofibers were estimated by section profiles. The yields of the higher-order structures were:[e] ~20%. [f] ~100%. [g] ~100%. [h] ~20%.

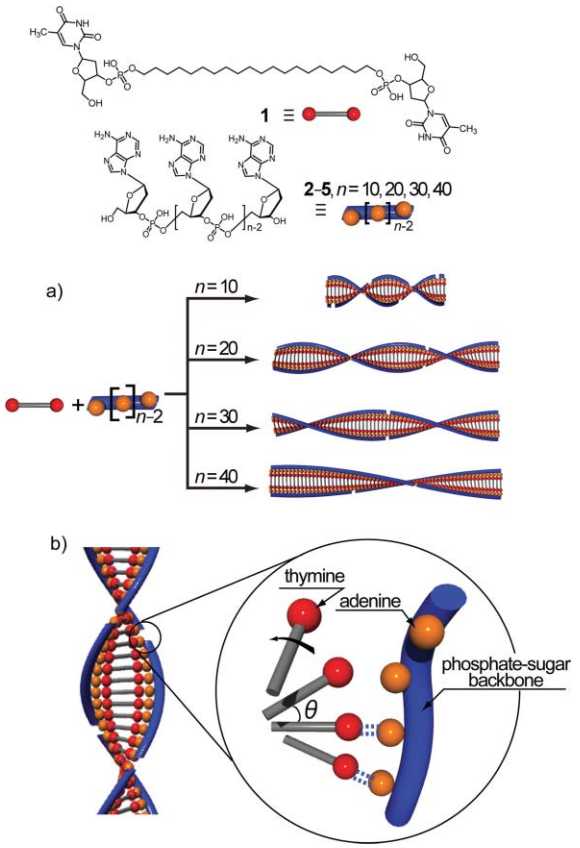

Fig. 7 Schematic illustrations of the proposed structures for (a) the binary self-assemblies of **1** and oligoadenylic acids **2–5** and (b) "end fraying" in the nanofiber structure. The increase in the deviation angle θ is induced by both the increase in mobility of the nucleotide terminus and the repulsion between the phosphate moieties.

longer templates, and this fraying should lead to more base-pair breaking between the thymine in **1** and the adenine in **2** (Fig. 7b). Once the hydrogen bonds between the base pairs are broken, it is likely that the free **1** molecules become more mobile and move away from each other because of the electrostatic repulsion between the phosphate groups. The resulting increase in the deviation angle θ between free **1** molecules leads to the formation of short-pitch helical nanofibers, as observed in **1/2**. Hillary *et al.* found that curved DNA is bent at the oligod(A)·d(T) sequence, in which the A–T base pairs have a large propeller twist.[30] Interestingly, the CD spectrum of **1/2** suggests that there is a large propeller twist in the A–T base pair and that the self-assembled nanofibers curve to form wavy morphologies. The nanofibers obtained from **1/2** also have many nicks, indicating the comparative flexibility of the fibers.

The helical nanofibers self-assembled from **1** and **4**, **7**, and **8** produced higher-order structures such as stranded ropes, whereas binary self-assemblies **1/3** and **1/5** retained helical nanofiber structures. We assume that the aging period allowed two helical nanofibers with narrow pitches (11 nm) to self-assemble into a double-stranded rope with a 100 nm pitch (Fig. 8). The CD spectrum of **1/4** differs from the spectra of **1/3** and **1/5**, which suggests the different molecular orientation of the nucleobase moiety. In addition, the hypochromicity of the absorption maxima

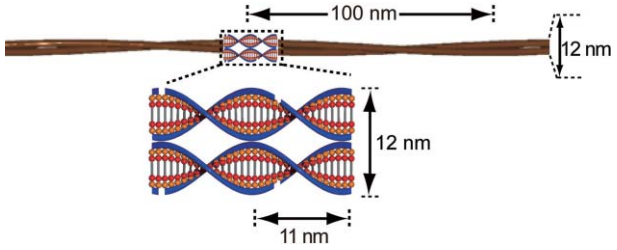

Fig. 8 Schematic illustration of the higher-order structure (a double-stranded rope) that formed from the binary self-assembly of **1** and **4**.

for **1/4** in the UV-vis spectrum (Fig. 3b) supports more effective stacking of the nucleotide moieties.

Experimental

General

Bolaamphiphile **1** was synthesized using the phosphoramidate method, as reported previously.[22] Synthetic oligoadenylic acids **2–8** were purchased from Fasmac Co. Compound **1** was dissolved in a 0.1× TE buffer solution by sonication for 1 h. Single-stranded oligoadenylic acids **2–8** were added to the solution of **1**, and the resultant mixture was kept at room temperature. The final concentrations of **1**, **2**, **3**, **4**, **5**, **6**, **7**, and **8** were adjusted to 1.8×10^{-2}, 1.8×10^{-3}, 9.0×10^{-4}, 6.0×10^{-4}, 4.5×10^{-4}, 1.8×10^{-3}, 1.8×10^{-3}, and 9.0×10^{-4} mol dm^{-3}, respectively, in order to complex thymine with adenine completely.

Atomic force microscopy (AFM)

A drop of each of the aqueous solutions obtained from the binary self-assembly of **1** and **2–8** was placed on a highly oriented pyrolytic graphite (HOPG) and dried for a few minutes. The specimen was then washed with excess pure water and dried with filter paper. The AFM images were obtained with a Nanoscope III (Veeco Instruments Inc.) using a silicon-micro cantilever (spring constant 2 N m^{-1}, frequency ≈ 70 kHz, Olympus) in a tapping mode.

UV-vis and CD spectroscopy

UV-vis and CD spectra were measured with UV-3100 (Shimadzu Corp.) and J-820 (JASCO Corp.) instruments, respectively, in 0.1× TE buffer solutions at 20 °C in a 0.01 cm quartz cell. The concentrations of the binary self-assemblies were adjusted to $2.6 \times 10^{-3}/2.6 \times 10^{-4}$, $2.6 \times 10^{-3}/1.3 \times 10^{-4}$, $2.6 \times 10^{-3}/8.7 \times 10^{-5}$, and $2.6 \times 10^{-3}/6.5 \times 10^{-5}$ mol dm^{-3} for **1/2**, **1/3**, **1/4**, and **1/5**, respectively. The spectra were measured 24 h after sample preparation.

Conclusion

We analyzed the morphologies of nanofibers self-assembled from nucleotide bolaamphiphile **1** with oligoadenylic acids of various lengths (**2–5**) and various oligonucleotide sequences (**6**, **7**, and **8**). The helical pitch of the resultant nanofibers depended strongly on the length of template oligoadenylic acids **2–5**. Slight changes in the propeller twist, nucleobase stacking, or flexure of the oligonucleotide were shown to influence the pitch and higher-order

self-assembled structures of the binary self-assemblies. We hope these results will greatly contribute to the construction and control of well-defined DNA-based nanomaterials using molecular recognition.

References

1 T. Park and S. C. Zimmerman, *J. Am. Chem. Soc.*, 2006, **128**, 14236–14237; T. Park and S. C. Zimmerman, *J. Am. Chem. Soc.*, 2006, **128**, 11582–11590; O. A. Scherman, G. Ligthart, R. P. Sijbesma and E. W. Meijer, *Angew. Chem., Int. Ed.*, 2006, **45**, 2072–2076.

2 Y. Kamikawa, M. Nishii and T. Kato, *Chem.–Eur. J.*, 2004, **10**, 5942–5951; T. Kato, N. Mizoshita and K. Kishimoto, *Angew. Chem., Int. Ed.*, 2006, **45**, 38–68.

3 E. Kolomiets, E. Buhler, S. J. Candau and J. M. Lehn, *Macromolecules*, 2006, **39**, 1173–1181; T. Sugimoto, T. Suzuki, S. Shinkai and K. Sada, *J. Am. Chem. Soc.*, 2007, **129**, 270–271.

4 T. Shimizu, *Macromol. Rapid Commun.*, 2002, **23**, 311–331; T. Shimizu, M. Masuda and H. Minamikawa, *Chem. Rev.*, 2005, **105**, 1401–1444.

5 M. C. T. Fyfe and J. F. Stoddart, *Acc. Chem. Res.*, 1997, **30**, 393–401; J.-M. Lehn, *Supramolecular Chemistry*, VCH, Weinheim, 1995; S. Sivakova and S. J. Rowan, *Chem. Soc. Rev.*, 2005, **34**, 9–21; S. Sivakova, J. Wu, C. J. Campo, P. T. Mather and S. J. Rowan, *Chem.–Eur. J.*, 2006, **12**, 446–456; F. Zeng and S. C. Zimmerman, *Chem. Rev.*, 1997, **97**, 1681–1712.

6 H.-J. Kim, W.-C. Zin and M. Lee, *J. Am. Chem. Soc.*, 2004, **126**, 7009–7014; L. Brunsveld, J. Vekemans, J. Hirschberg, R. P. Sijbesma and E. W. Meijer, *Proc. Natl. Acad. Sci. U. S. A.*, 2002, **99**, 4977–4982.

7 S. J. George, A. Ajayaghosh, P. Jonkheijm, A. Schenning and E. W. Meijer, *Angew. Chem., Int. Ed.*, 2004, **43**, 3422–3425.

8 T. Kawasaki, M. Tokuhiro, N. Kimizuka and T. Kunitake, *J. Am. Chem. Soc.*, 2001, **123**, 6792–6800.

9 I. Koltover, T. Salditt, J. O. Radler and C. R. Safinya, *Science*, 1998, **281**, 78–81; J. O. Radler, I. Koltover, T. Salditt and C. R. Safinya, *Science*, 1997, **275**, 810–814.

10 E. Braun, Y. Eichen, U. Sivan and G. Ben-Yoseph, *Nature*, 1998, **391**, 775–778.

11 S. H. Park, P. Yin, Y. Liu, J. H. Reif, T. H. LaBean and H. Yan, *Nano Lett.*, 2005, **5**, 729–733; H. Yan, S. H. Park, G. Finkelstein, J. H. Reif and T. H. LaBean, *Science*, 2003, **301**, 1882–1884.

12 K. Tanaka, A. Tengeiji, T. Kato, N. Toyama and M. Shionoya, *Science*, 2003, **299**, 1212–1213.

13 C. A. Mirkin, R. L. Letsinger, R. C. Mucic and J. J. Storhoff, *Nature*, 1996, **382**, 607–609.

14 J. L. Czlapinski and T. L. Sheppard, *J. Am. Chem. Soc.*, 2001, **123**, 8618–8619; J. L. Czlapinski and T. L. Sheppard, *Bioconjugate Chem.*, 2005, **16**, 169–177.

15 S. Vogel, K. Rohr, O. Dahl and J. Wengel, *Chem. Commun.*, 2003, 1006–1007.

16 K. V. Gothelf and R. S. Brown, *Chem.–Eur. J.*, 2005, **11**, 1062–1069; K. V. Gothelf, A. Thomsen, M. Nielsen, E. Clo and R. S. Brown, *J. Am. Chem. Soc.*, 2004, **126**, 1044–1046.

17 K. Sugiyasu, M. Numata, N. Fujita, S. M. Park, Y. J. Yun, B. H. Kim and S. Shinkai, *Chem. Commun.*, 2004, 1996–1997; M. Numata and S. Shinkai, *Chem. Lett.*, 2003, **32**, 308–309.

18 P. G. A. Janssen, J. Vandenbergh, J. L. J. vanDongen, E. W. Meijer and A. P. H. J. Schenning, *J. Am. Chem. Soc.*, 2007, **129**, 6078–6079.

19 R. Iwaura, F. J. M. Hoeben, M. Masuda, A. Schenning, E. W. Meijer and T. Shimizu, *J. Am. Chem. Soc.*, 2006, **128**, 13298–13304.

20 R. Iwaura, K. Yoshida, M. Masuda, M. Ohnishi-Kameyama, M. Yoshida and T. Shimizu, *Angew. Chem., Int. Ed.*, 2003, **42**, 1009–1012.

21 R. Iwaura, M. Ohnishi-Kameyama, M. Yoshida and T. Shimizu, *Chem. Commun.*, 2002, 2658–2659.

22 R. Iwaura, K. Yoshida, M. Masuda, K. Yase and T. Shimizu, *Chem. Mater.*, 2002, **14**, 3047–3053.

23 T. Itahara, *Bull. Chem. Soc. Jpn.*, 1997, **70**, 2239–2247; D. T. Browne, J. Esinger and N. J. Leonard, *J. Am. Chem. Soc.*, 1968, **90**, 7302–7323; S. Aoyagi and Y. Inoue, *J. Biol. Chem.*, 1968, **243**, 514–520; M. M. Warshaw and I. Tinoco, *J. Mol. Biol.*, 1966, **20**, 29–38.

24 D. M. Gray, K. H. Johnson, M. R. Vaughan, P. A. Morris, J. C. Sutherland and R. L. Ratliff, *Biopolymers*, 1990, **29**, 317–323; S. Brahms and J. G. Brahms, *Nucleic Acids Res.*, 1990, **18**, 1559–1564.

25 S. R. Gudibande, S. D. Jayasena and M. J. Behe, *Biopolymers*, 1988, **27**, 1905–1915.

26 A. L. Williams, C. Cheong, I. Tinoco and L. B. Clark, *Nucleic Acids Res.*, 1986, **14**, 6649–6659.

27 L. E. Ulanovsky and E. N. Trifonov, *Nature*, 1987, **326**, 720–722; H. S. Koo, H. M. Wu and D. M. Crothers, *Nature*, 1986, **320**, 501–506; P. J. Hagerman, *Nature*, 1986, **321**, 449–450.

28 I. Tinoco, *J. Am. Chem. Soc.*, 1964, **86**, 297–298.

29 S. Nonin, J. L. Leroy and M. Gueron, *Biochemistry*, 1995, **34**, 10652–10659; J. L. Leroy, M. Kochoyan, T. Huynhdinh and M. Gueron, *J. Mol. Biol.*, 1988, **200**, 223–238; S. R. Holbrook and S. H. Kim, *J. Mol. Biol.*, 1984, **173**, 361–388; D. Andreatta, S. Sen, J. L. PerezLustres, S. A. Kovalenko, N. P. Ernsting, C. J. Murphy, R. S. Coleman and M. A. Berg, *J. Am. Chem. Soc.*, 2006, **128**, 6885–6892.

30 C. M. Hillary, H. C. M. Nelson, J. T. Finch, B. F. Luisi and A. Klug, *Nature*, 1987, **330**, 221–226.